High porosity activated carbon synthesis using asphaltene particles

Muwafaq Ayesh Rabeea, Tahseen Ali Zaidan, Abdalkareem Hamad Ayfan & Atyaf A. Younis

Carbon Letters

ISSN 1976-4251

Carbon Lett.
DOI 10.1007/s42823-019-00086-0

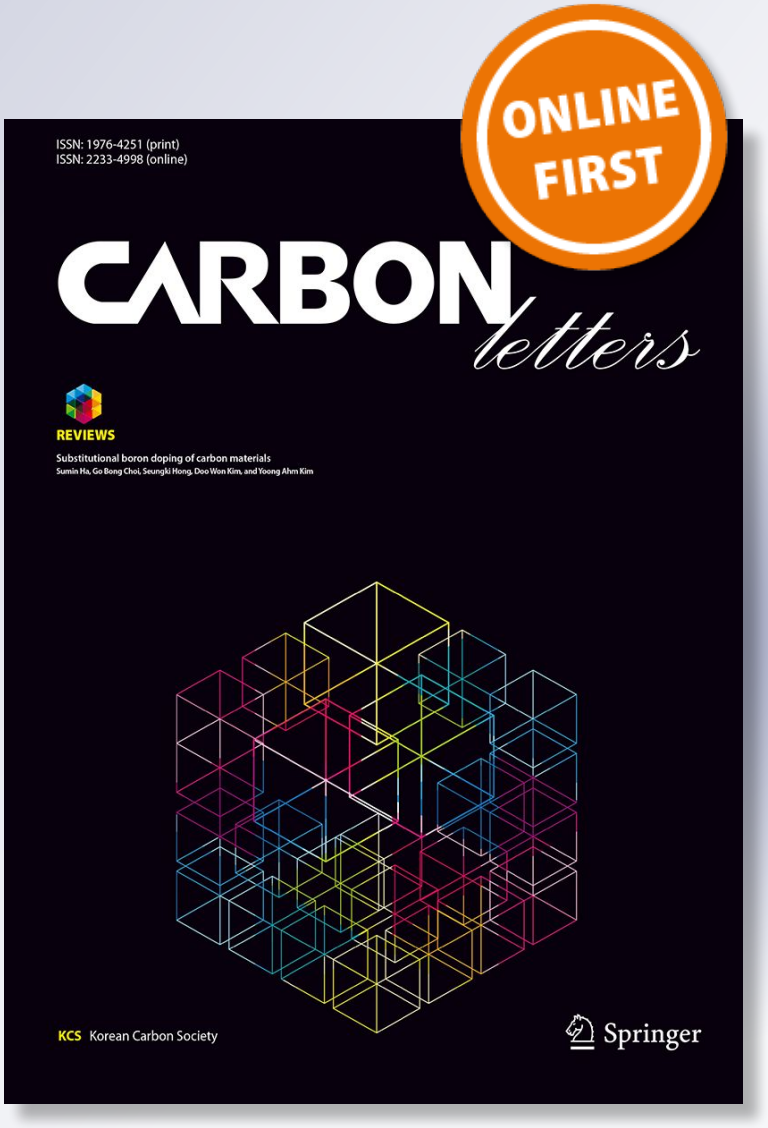

Springer

Carbon Letters
https://doi.org/10.1007/s42823-019-00086-0

Online ISSN 2233-4998
Print ISSN 1976-4251

ORIGINAL ARTICLE

High porosity activated carbon synthesis using asphaltene particles

Muwafaq Ayesh Rabeea[1] · Tahseen Ali Zaidan[1] · Abdalkareem Hamad Ayfan[2] · Atyaf A. Younis[1]

Received: 30 April 2019 / Revised: 2 August 2019 / Accepted: 9 August 2019

Abstract
The study aims to use asphaltene particles (As) extracted from natural bitumen to synthesize activated carbon (ACAs). The asphaltene particles were mixed with a fixed weight of potassium hydroxide (KOH) as an activating agent, preheated to 600 °C, and then treated with 15% hydrofluoric acid (HF). The methylene blue (MB) 20 mg/l was used to determine the adsorption capacity of ACAs and reactivated carbon (RACAs). The morphology of ACAs and its components were characterized using scanning electron microscopy–energy dispersive X-ray (SEM–EDX) and Fourier-transform infrared spectroscopy (FTIR). The study included the application of adsorption isotherms Freundlich and Langmuir on the experimental data of the studied systems. The yield of ACAs was 92% of the raw material. The activated carbon displayed high adsorption capacity and can be reprocessed after reactivation using microwave radiation. The active surface area of ACAs is found to be 970 m^2/g. The effectiveness and adsorption ability of ACAs and RACAs, as proven by its adsorption capacity (218.15 and 217.907 mg/g) for MB, demonstrate that ACAs and RACAs have a large external surface area and an extensive array of pores. The ACAs are most sensitive at 30 °C and neutral pH. The results also showed that the isotherms have a good fit to the experimented data.

Keywords Asphaltene · Activated carbon · Reactivation · Adsorption isotherm · Microwave

1 Introduction

The elimination or reduction of pollutants and toxic substances via different industrial processes has evolved into an important issue that currently confronts the environment and society [1]. Adsorption on solid surfaces is effective for the removal and treatment of contaminants. Adsorption is defined as a phenomenon that involves the accumulation of molecules, atoms or ions (adsorbent substance) on the surface of the adsorbent substance. Activated carbon is an important material competing in the field of adsorbing pollutants [2–6]. Several studies have explored the preparation and synthesis of activated carbon from different materials, although carbon is a basic atom in its composition. The morphology and characteristics of activated carbon have been studied. Activated carbon is a highly porous material with a wide array of shapes and sizes of these pores, resulting in its varied uses and applications. The nonpolar nature of activated carbon allows for the interaction between its porous structures and the adsorption process [2].

The activated carbon is used for the treatment of portable and industrial water due to its ability to eradicate odors, colors, and contaminants [7]. Furthermore, activated carbon is used to adsorb pollutants, toxic gases, pigments, liquid purification, and heavy metals [8–10]. The properties of activated carbon are dependent on several factors that include the precursor raw material, the carbonization process and the activation method [11]. Activated carbon can be obtained from various raw materials (bitumen, coal, wood, coconut husks, and other organic materials) using the carbonization process. The carbonization temperature ranges from 500 to 950 °C and the weight loss of raw materials denotes the presence of volatiles [12, 13]. Teng prepared highly adsorptive activated carbon from bitumen, extracted from crude oil, using H_3PO_4 as activated agent, and then subjected to carbonization at 600 °C for 3 h [14]. Munther et al. synthesized activated carbon from bituminous and studied the effect of pH on the absorbance characteristic [15]. Also, Muwafaq et al prepared activated carbon using bitumen modified by

✉ Muwafaq Ayesh Rabeea
muw88@uoanbar.edu.iq

[1] Department of Ecology, College of Applied Sciences, University Of Anbar, Hit, Anbar 31001, Iraq

[2] College of Pharmacy, University Of Anbar, Ramadi, Anbar, Iraq

Published online: 22 August 2019

waste polymers and investigated its absorbance efficiency using methylene blue and iodine number [16]. Rasim et al. [17] synthesized activated carbon from natural bitumen via chemical activation (KOH).

Bitumen is defined as the residual non-destructive distillation product of crude oil or a derivative of the treatment of crude oil with some organic solvents. In some countries, bitumen is a natural sedimentation product that results from the rise of crude oil in the earth's surface, and then subjected to climatic influences and oxidation for extended periods [18]. Asphaltene is the heaviest among various components of bitumen and can be obtained from precipitation in the presence of *n*-alkanes. [19].

Natural bitumen in western Iraq contains a high percentage of As (40%), since it suffers through the process of natural oxidation. In this paper, As is used to synthesize activated carbon with high yield and quality. On the other hand, this study sheds the light on using abundant and cheap natural materials to prepare activated carbon which can then be used to control environmental pollutants.

2 Experiments

2.1 Materials

The asphaltene particles (As) with normal hexane (1:40 w/v bitumen:solvent) were extracted from natural bitumen (As, 40%) obtained in the west of Iraq by continuous stirring in 0 °C for 3 h. Afterwards, the particles were filtered and dried at 100 °C. The methylene blue (MB) used in this study, manufactured by Hopkin & Williams Company, has a chemical formula of $C_{16}H_{18}N_3$ and molecular weight of 319.85 g/mol.

2.2 Preparation of activated carbon (ACAs and RACAs)

The process of ACAs preparation starts by mixing As with KOH (1:2 w/w) in a crucible that is tightly sealed with heat-resistant aluminum foil. The crucible is then gradually heated in a muffle furnace, increasing the temperature in steps of 10 °C per min. The carbonization process was sustained for 3 h as the temperature reached 600 °C. The carbonated material was collected and cooled to room temperature. Afterwards, the sample was washed with distilled water to ensure the neutralization of pH. The ACAs were subsequently refluxed with 15% HF for 5 h, and subjected to direct filtration and washing with distilled water to re-neutralize the pH. The ACAs were dried using an electric oven at 110–120 °C for 24 h, and then sieved to 100 µm. After that, the used ACAs were recovered and reactivated using 10% HCl and microwave radiation at a power of 500 watts for 15 min. The reactivated carbon (RACAs) were then filtered, washed with distilled water for pH reneutralization, and dried at 110–120 °C for 24 h.

2.3 Adsorption properties

The concentration of MB, removed from its aqueous solution, was calculated using UV–Vis type of T80 UV/Vis spectrometer. IR (BRUKER) was used to analyze the functional groups in As and ACAs within the scanning range of 400–4000/cm. The morphology and components of ACAs were characterized using SEM–EDX. The active surface area of the ACAs was calculated by exposing the ACAs to nitrogen gas (single-point BET analysis). The physical properties of the synthesized ACAs (yield, moisture content and ash content) were determined using ASTM standard techniques.

2.4 Adsorption isotherms

To determine the adsorbent dose, the ACAs were divided into specific masses of 0.005, 0.01 and 0.05 g and poured into three conical flasks. 110 ml of MB solution (20 mg/l) was then added to each flask. The resulting solution was continuously stirred for 30 min at 30 °C and neutral pH. The solution contained in each flask was centrifuged at 5000 r/min for 5 min. The absorbance of the residual solution was measured using UV–Vis at λ_{max} of 665 nm. The concentration and adsorption capacity of adsorbed MB were calculated using the following equation:

$$q_e = (C_i - C_e) \times V/M, \tag{1}$$

where q_e denotes adsorption capacity in (mg/g), C_i represents the initial concentration in the MB (mg/g), C_e signifies equilibrium liquid phase concentration in (mg/g), V symbolizes the volume of the solution in (L) and M is the mass of dry adsorbent in (g).

To study the effect of temperature on the morphology and adsorption capacity of ACAs, 0.01 g of ACAs was separated into four conical flasks that contain 110 ml of MB solution (20 mg/l). The mixture was stirred for 30 min at 20, 30, 40 and 50 °C, and neutral pH. The solution of each flask was centrifuged at 5000 r/min for 5 min and the absorbance of the residual solution was measured using UV–Vis at λ_{max} 665 nm. To determine the effect of concentration, 110 mL of different concentrations of MB 20, 30, 40 and 50 mg/l was stirred with 0.01 g of ACAs for 30 min at 30 °C and neutral pH. Afterwards, each solution was centrifuged at 5000 r/min for 5 min. The contact time (10, 20, 30, 40, 50 min) effect is evaluated under certain circumstances (110 ml of MB solution (20 mg/l), 30 °C temperature, neutral pH, and 0.01 g of ACAs).

The adsorption efficiency and capacity were also determined by applying Langmuir and Freundlich isotherms to the experimental data of MB adsorption using Eqs. 3 and 4.

3 Result and discussion

The physical properties of the synthesized ACAs are presented in Table 1, which shows that the yield of ACAs is 92%. This is apparent as As are a well-known carbon matter with some other metal constituents [20]. Elucidating the transformation of a large raw material into ACAs is important, since the losses during the preparation at high temperatures can produce harmful residual pollutants, which can affect workers and the environment. In addition, the losses retain some of the raw material, thus they must be reduced to a minimum.

Table 1 shows that the prepared ACAs exhibits less moisture content (1.4%) than the TIGG commercial activated carbon (2%). The low ash content (0.6%) indicates that the ACAs are stable. This low percentage can be attributed to the HF (10%) dissolution of the residual components associated with ACAs. The reactivation of ACAs is via microwave radiation and the use of HCl acid (10%). This reactivation feature allows the multiple use of ACAs in a straightforward, cost-effective and innocuous way.

The pores' volume of the synthesized ACAs is 1.31 cm^3/g, whereas the active surface area (refers to the adsorption quality of Nitrogen gas) is found to be 970 m^2/g as shown in Table 1. The activated carbon effectivity to adsorb nitrogen gas is related directly to the pores of the activated carbon and their internal surface area. Therefore, if pores are bigger, so is the active area (Fig. 2), which enables the synthesized material to be actively used to control the gas pollutants harming the environment.

The effectiveness and adsorption ability of ACAs, as proven by its adsorption capacity (218.15 mg/g) for MB, demonstrate that ACAs have a large external surface area and an extensive array of pores. Therefore, ACAs can adsorb more contaminants and particles that have large molecular weights such as MB.

Figure 1a illustrates that increasing the dose of adsorbent leads to increasing the adsorption efficiency because of the increase in the adsorption sites. With a constant concentration of dye, the adsorption capacity is reduced, since it spreads out to more active adsorption sites.

In Fig. 1b, high dye concentration leads to less adsorption efficiency but more adsorption capacity. High concentration means more dye particles can be adsorbed on the ACAs until the active sites reach saturation. However, a lack of more dye particles is still observed in the solution causing a lack of adsorption efficiency [21].

Time is an effective factor in controlling the disposal of pollutants prior to attaining the critical concentration. The results in Fig. 1c refer to adsorption occurring rapidly at the beginning of the process, then the ACAs reach equilibrium at 30 min when most of adsorption sites reach saturation. Then, the free dyes compete with the absorbed dyes on the ACAs which leads to decrease the adsorption until the equilibrium taken place. The MB removal percentage is calculated using Eq. 2.

$$\text{Adsorption} = \frac{C_i - C_e}{C_i} \times 100. \tag{2}$$

The optimal adsorption performances of ACAs and RACAs were achieved at 30 °C, as shown in Fig. 1d. Maintaining the temperature above 30 °C results in the expulsion of MB from the ACAs pores (desorption) to the solution, since the absorption of ACAs has been a physical nature attributed to the weak binding force between the chemical substance and adsorbent surface which can be broken by increasing the kinetic energy of the MB by raising its MB particles temperature [22, 23] (see Table 2).

3.1 Characterization of the adsorbents

SEM images shown in Fig. 2 demonstrated a wide array of pores with a diameter that ranged from 1.4 to 4.5 µm on the external surface of ACAs. It should be mentioned that there are a few pores with diameters less than 1.4 µm. The uniform distribution of pores is attributed to high and fast adsorption of MB on the ACAs (Fig. 2b). This good result is due to the use of KOH as a chemical reagent to aid the development of pores on the surface of the carbon material [24]. The EDX analysis (Table 1) indicates the prepared material constitutes 96.52% of carbon atoms. Unfortunately, 0.6% of zirconium ions is denoted using the crucible in the carbonization process, where the percentage composition of nitrogen and sulfur atoms is 0.48 and 2. 4, respectively. This proves that chemical and physical adsorptions may occur simultaneously on the surface of ACAs. The absorption of activated carbon is dependent on the chemical composition of the liquid and solid phases [25]. The reactivation process was performed using microwave radiation and HCl to achieve a fully chemical adsorption removal (for getting RACAs).

The IR spectrum (Fig. 3a) shows there are two packages of the As molecules: the peak at 805/cm, which is attributable to the synergy between the carbon and silicon of the

Table 1 Physical properties of ACAs (%)

Yield	Ash content	Moisture content	Active surface area	Pore volume	C	S	N	Zr
92	0.6	1.4	970 m^2/g	1.31 cm^3/g	96.52	2.4	0.48	0.6

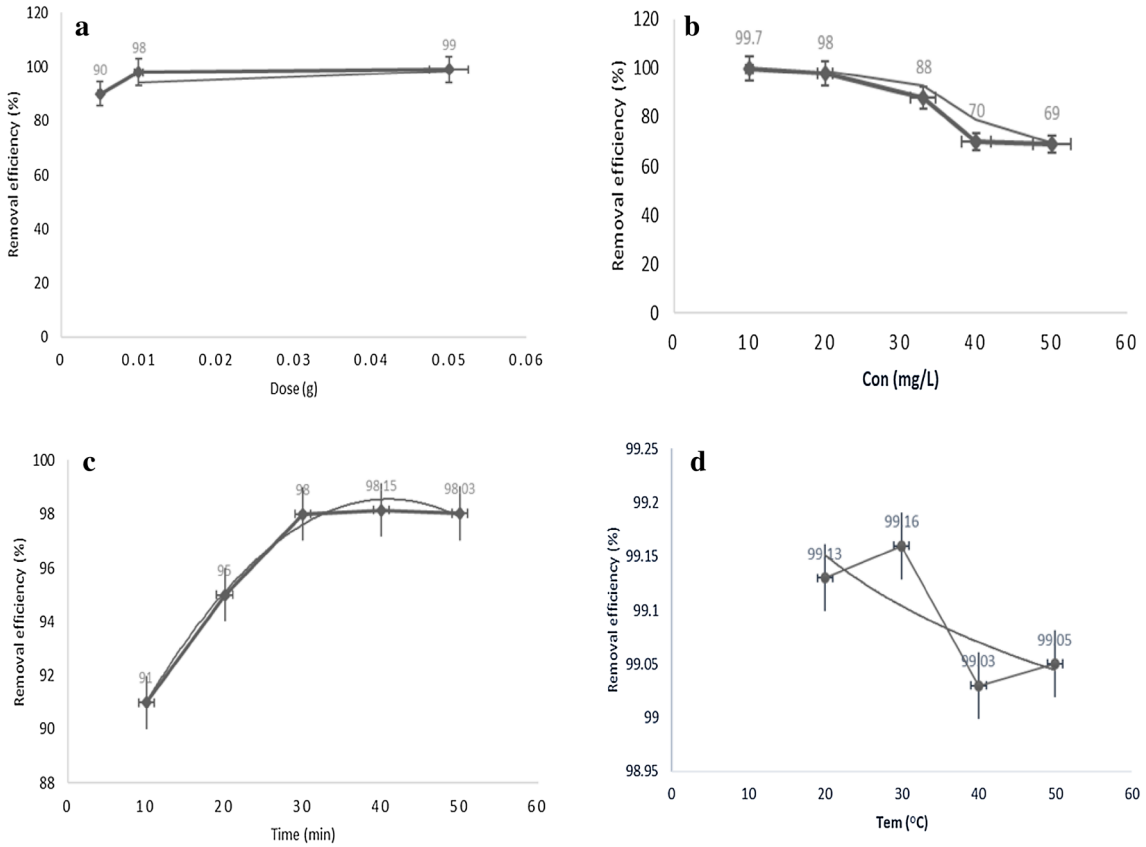

Fig. 1 Effect of **a** dose, **b** concentration (Con), **c** time, and **d** temperature (Tem) on adsorption efficiency

Table 2 Effect of temperatures on MB adsorption capacity onto ACAs and RACAs for 30 min in a neutral pH

Adsorbent	Temp (°C)	C_e (mg/g)	q (mg/g)
ACAs	20	0.1739	217.977
	30	0.16815	218.150
	40	0.193296	217.884
	50	0.19022	217.873
RACAs	30	0.1902	217.907

group (Si–C) and absorption band at 1136/cm denoting the oxygen bond in the Si–O. Two absorption bands were identified at 1375/cm and 1456/cm, indicating the homogeneous and heterogeneous bending vibration of the methylene group (CH_2) or the methyl (CH_3). The absorption bands at 2850/cm and 2920/cm are characteristic peaks of symmetric and asymmetric vibrations (CH_2). The four C–H groups are attributable to the methylene (CH_2) and methyl (CH_3) groups in the chemical structure of the As, which is proven by the occurrence of an absorption band at 1035/cm. Also observed in the spectrum is a distinct peak at 1607/cm that denotes the C=C vibration of successive double bonds in the aromatic rings.

The FTIR spectral results support the accurate chemical composition of the two substrates in the selected model [26]. The absorption band at 3100/cm is ascribed to the = C–H vibration of the aromatic compounds [27]. The band at 2522/cm confirms the occurrence of sulfur compounds (S–H group), while the absorption peak at 667/cm is indicative of the C–S group [28–30]. The absorption band at 1141/cm signifies the presence of nitrogen as the C–N group associated with carbon atoms in As. The absorption at 3346/cm also confirms the presence of nitrogen as the NH group [31–33].

The characteristic peaks of ACAs appear at 667/cm and at 722/cm (Fig. 3b), which result from the connection of the electron pairs of the sulfur and nitrogen atoms with the empty orbitals in the zirconium atoms. The disappearance of N–H group and S–H group is due to the expulsion of hydrogen atoms by heat. The absence of absorption bands denoting the silicon–carbon (Si–C) bond is due to the dissolution of silica by hydrofluoric acid (Fig. 3b).

3.2 Isotherms adsorption studies

The adsorption process is described by adsorption isotherms, which are based on theories that vary in line with the principle of each isotherm, and tested using experimental

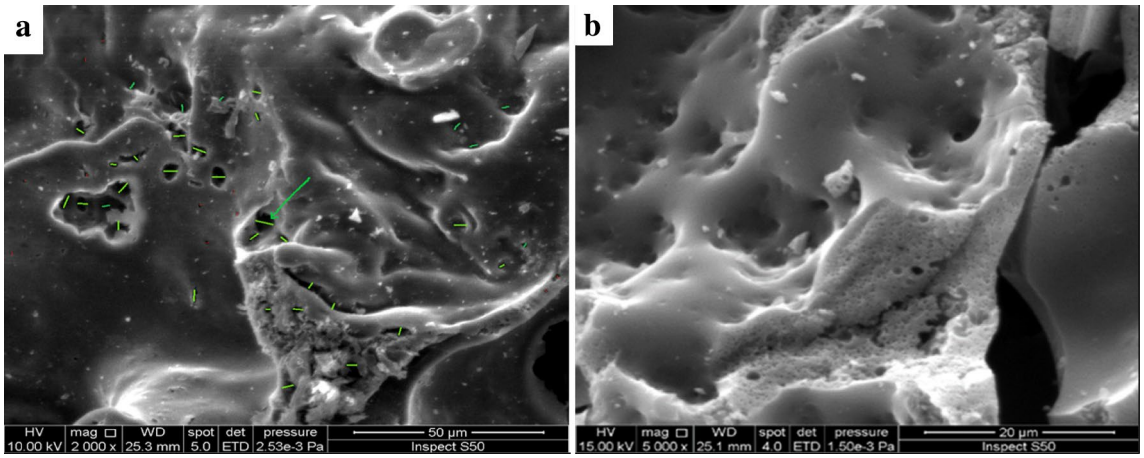

Fig. 2 SEM image of ACAs: **a** before adsorption MB and **b** after adsorption MB

data [34]. The Freundlich isotherm model indicates that the surface is almost entirely heterogeneous, which is denoted by irregular energy changes due to the varying energy levels of adsorption sites [35]. According to Eq. 3, the Freundlich isotherm is applied.

$$\mathrm{Log}q_e = \log K + 1/n \log C_e, \tag{3}$$

where K and n are Freundlich outcomes derived from the slope and intercept, respectively. These values are dependent on the nature and surface of the adsorbent.

On the other hand, Langmuir isotherm is pertinent to the description and study of the monolayer adsorption, which suggests that the energy is homogeneously distributed on the adsorbent surface [36, 37]. Langmuir isotherm shows the variation of C_e/q_e versus C_e based on Eq. 4. The Langmuir outcomes are represented by Q_{max} and b, which are derived from the slope and intercept, respectively.

$$\frac{C_e}{q_e} = \frac{1}{b} + \frac{C_e}{Q_{max}}, \tag{4}$$

where q_e denotes the adsorption capacity at equilibrium in mg/g, Ce represents the equilibrium concentration of MB in mg/L, Q_{max} signifies the theoretical maximum adsorbent capacity of MB on the surface of ACAs in mg/g, and b is the Langmuir outcomes in l/mg,

The amount of adsorbent is a key parameter in the adsorption study [38]. 0.01 g/l of ACAs was experimentally shown to be appropriate for absorption analysis using Langmuir and Freundlich isotherms. It was selected because it achieves an acceptable equilibrium ratio of the MB in aqueous solution. The experimental data are consistent with the Freundlich isotherm, since the extracted correlation coefficient value is approximately unity (0.9989). This implies that the adsorption on the surface of the ACAs is arbitrarily distributed on the external and internal pores and has not attained saturation state. Despite the low percentage of chemically adsorbed ions or compounds, the results indicate that physical adsorption on the ACAs is positive, since the value of n (1.769) is larger than unity ($1 < n$). In addition, K, which denotes the amount of MB adsorbed onto ACAs for a unit equilibrium concentration, is 159.074 (l/g) as shown in Table 3.

The Langmuir isotherm is confirmed by the linear relationship of Langmuir equation and the values of correlation coefficient (0.9816) as shown in Table 3. This indicates that adsorption ultimately reverts to a regular behavior to form a monolayer on the outer surface of ACAs, as shown in Fig. 2b. The b value (0.22) is related to the power of MB cohesion to the surface, which supports the physical behavior of the studied adsorption system. The Q_{max} value (769.23 mg/g) confirms the ability of the ACAs to adsorb additional quantities of MB from the aqueous solution. The R_L values range between 0.185 and 0.083 ($0 < R_L < 1$), which implies that the adsorption on the ACAs was favorable under the conditions selected for this study (Table 3).

R_L is a dimensionless equilibrium parameter that can be expressed in the equation below:

$$R_L = 11 + bC_0, \tag{5}$$

where b is the Langmuir constant and C_0 represents the critical concentration of MB (mg/l).

4 Conclusions

To effectively exploit the benefits of natural bitumen, its high percentage of As can be controlled using activated carbon. The effectiveness and adsorption ability of ACAs, as proven by its adsorption capacity (218.15 mg/g) for MB, demonstrate it has a large external surface area and an extensive

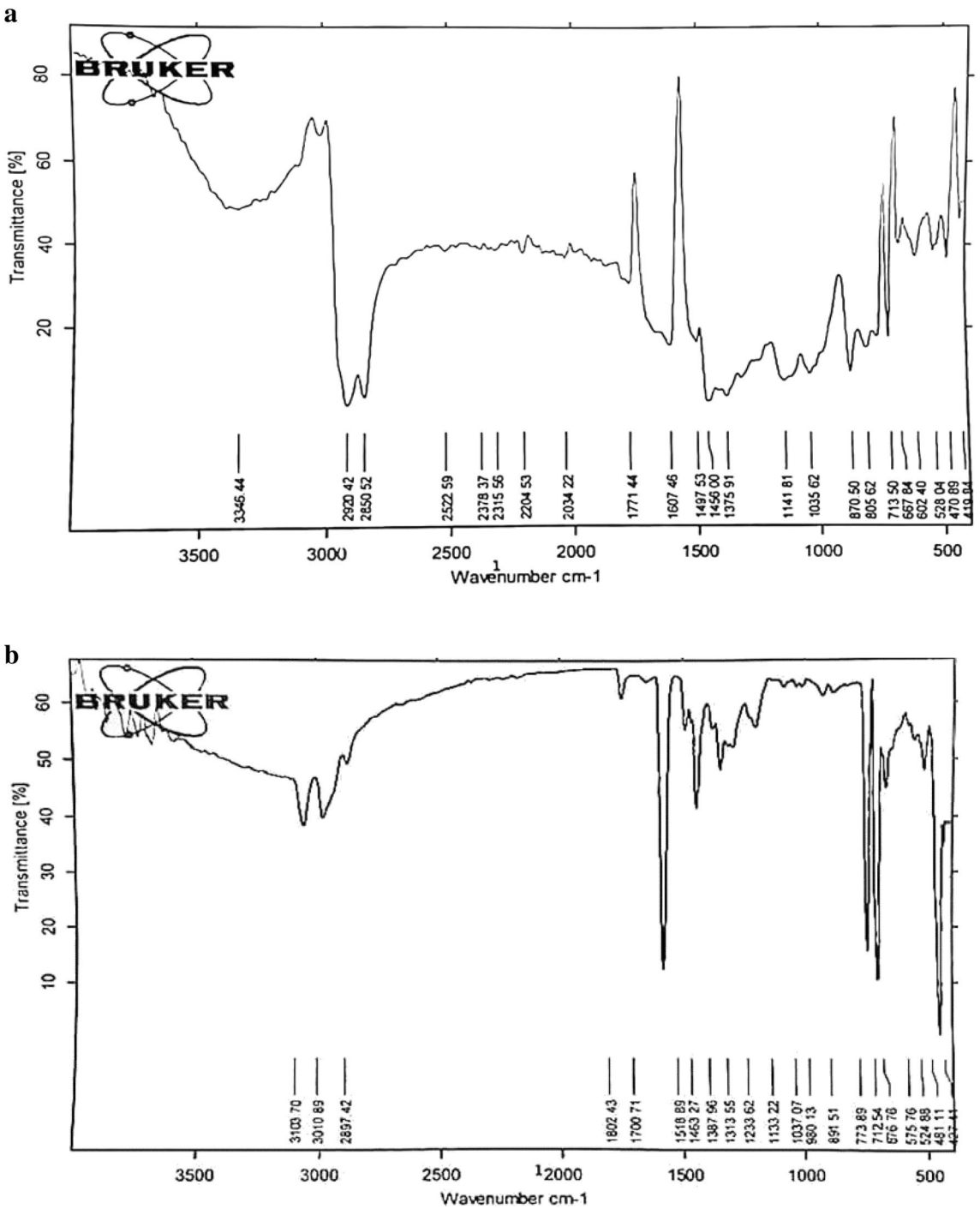

Fig. 3 FTIR spectra of asphaltene (As) particular (**a**). FTIR spectra of ACAs (**b**)

Table 3 Parameters of Langmuir and Freundlich isotherms

Adsorbate	Langmuir				Freundlich		
	Q_{max} (mg/g)	b	R^2	R_L	K (l/g)	n	R^2
ACAs	769.23	0.220	0.9816	0.185–0.083	159.074	1.769	0.9989

array of pores. Thus, ACAs can adsorb more contaminants and particles that have large molecular weights such as MB. The used ACAs are reactivated using HCl and microwave radiation to get its maximum benefit. The results have shown that ACAs and RACAs can be very active at 30 °C and neutral pH. Thus, the production process of the proposed ACAs is economically effective.

References

1. Bhuvan S, Govinda P (2018) The threat of ambient air pollution in Kathmandu, Nepal. J Environ Public Health. https://doi.org/10.1155/2018/1504591 **(Article ID 1504591)**
2. Kumar A, Mohan HJ (2016) Preparation and characterization of high surface area activated carbon from Fox nut (*Euryale ferox*) shell by chemical activation with H_3PO_4. Results Phys 6:651
3. Ying L, Xiaohui L, Wenping D et al (2017) Efficient adsorption of sulfamethazine onto modified activated carbon: a plausible adsorption mechanism. Sci Rep 7:12437
4. Kim Y, Kim JH, Lee KG, Kang SG (2005) Adsorption behavior of heavy metal ions in the solution of clay minerals under various conditions. J Ceram Process Res 6:25
5. Simone C, Marco C (2018) Modeling the adsorption equilibrium of small-molecule gases on graphene: effect of the volume to surface ratio. Phys Chem Chem Phys 20:9770
6. Dąbrowski A (2001) Adsorption—from theory to practice. Adv Coll Interface Sci 93:135
7. Sara D, Tushar S (2014) Review on dye removal from its aqueous solution into alternative cost effective and non-conventional adsorbents. J Chem Process Eng 1:1–11
8. George T, Simona M, Katerina S, Peter T, Tony S (2016) Mechanochemical and chemical activation of lignocellulosic material to prepare powdered activated carbons for adsorption applications. Powder Technol 299:41
9. Ali HJ, Ramlah AR, Mohd AM, Lee DW (2016) Adsorption of methylene blue onto activated carbon developed from biomass waste by H_2SO_4 activation: kinetic, equilibrium and thermodynamic studies. Desalin Water Treat 57:1
10. Guliyev NG, Ibrahimov HJ, Alekperov JA et al (2018) Investigation of activated carbon obtained from the liquid products of pyrolysis in sunflower oil bleaching process. Int J Ind Chem 9:277. https://doi.org/10.1007/s40090-018-0156-1
11. Hai NT, You SJ, Huan-Ping C (2017) Fast and efficient adsorption of methylene green 5 on activated carbon prepared from new chemical activation method. J Environ Manag 188:322
12. Dı´az-Tera´n J, Nevskaia DM, Lo´pez-Peinado AJ (2001) Porosity and absorption properties of an activated charcoal. Colloids Surface A Physiochem Eng Aspects 187:167
13. Fu K, Yue Q, Gao B et al (2017) Activated carbon from tomato stem by chemical activation with $FeCl_2$. Colloids Surf A 529:842
14. Teng HS, Yeh TS, Hsu LY (1998) Preparation of activated carbon from bituminous coal with phosphoric acid activation. J Carbon 36:1387
15. Munther IK, Reyad S, Mahmoud A (2006) Synthesis and characterization of activated carbon from asphalt. Appl Surf Sci 253:821
16. Muwafaq AR, Rasim FM, Atyaf AY (2017) Preparation activated carbon from Biji refinery asphalt treated with sulfur and waste polymers. Int J Appl Eng Res 12:14783
17. Rasim FM, Muwafaq AR, Thsin AZ (2019) Properties improvement of activated carbon prepared from Hit natural asphalt by phenol formaldehyde polymer waste. Res J Pharm Technol 12(6):2955–2958
18. Simon IA, James GS (2001) Petroleum resins: separation, character, and role in petroleum. Pet Sci Technol 19:1–2. https://doi.org/10.1081/LFT-100001223
19. James GS (2004) Petroleum asphaltenes—part 1: asphaltenes, resins and the structure of petroleum. Oil Gas Sci Technol 59:467
20. Zhen B, Ali Q, Atena S et al (2018) Asphaltene deposition during bitumen extraction with natural gas condensate and naphtha. Energy Fuels 32:1433
21. Hesas RH, Arami-Niya et al (2013) Preparation and characterization of activated carbon from apple waste by microwave –assisted phosphoric acid activation: application methylene blue adsorption. Bio Resour 8:2950
22. Al-Hyali OM, Ramadhan SA (2005) Effect of substantiates types on the adsorption of aromatic carboxylic acid and their relation to concentration, temperature and pH. Raf J Sci 16:68
23. Marsh H, Rodriguez-Reinoso F (2006) Activated carbon, 1st edn. Elsevier Science and Technology Books, New York, p 27 **(183-186, 243-251)**
24. Kim JH, Hwang SY, Park JE et al (2019) Impact of the oxygen functional group of nitric acid-treated activated carbon on KOH activation reaction. Carbon Lett 29:281. https://doi.org/10.1007/s42823-019-00024-0
25. Steenberg B (1944) Adsorption and Exchange of Ions by Activated Charcoal. Uppsala, Almquist and Wiksells, Stockholm
26. Mistry B (2009) Handbook of spectroscopic data CHEMISTRY (UV, JR, PMR, JJCNMR and Mass Spectroscopy). Oxford Book Company, Oxford, pp 26–56
27. Lee SM, Bae BS, Park HW et al (2015) Characterization of Korean Red Ginseng (*Panax ginseng* Meyer): History, preparation method, and chemical composition. J Ginseng Res 39:384
28. Robert S, Francis W, David K (2005) Spectrometric identification of organic compounds, 7th edn. Wiley, Hoboken, pp 72–126
29. Kazuo N (2009) Infrared and raman spectra of inorganic and coordination compounds part A: theory and applications in inorganic chemistry, 6th edn. Wiley, Hoboken
30. Sev S, Field L, John K (2008) Organic structures from spectra, 4th edn. Wiley, Hoboken, pp 15–20
31. Obaid A, Hiba T, Rasim FM (2017) Synthesis and characterization of novel 1,3-oxazepine-5(1H)-one derivatives via reaction of imine compounds with isobenzofuran-1(3H)-one. Acta Pharm Sci 55:43
32. Rasim FM, Hiba T, Mustafa O, Obaid A (2018) Synthesis, characterization and evaluation of antifungal activity of seven-membered heterocycles. Acta Pharm Sci 56:39
33. Simek J (2013) Organic chemistry, 8th edn. Pearson education, Inc, London, pp 412–414
34. Kent SK (2003) Adsorbent selection, Adsorption research. Inc. Dubiln, ohio 43016:1–23
35. Freundlich H (1906) Uber die adsorption Isoungen. Z Phys Chem 57:385
36. Radushkevich LV (1974) Potential theory of sorption and structure of carbons. Zh Fiz Khim 23:1410
37. Wang Q, Fu F (2011) Removal of heavy metal ions from wastewaters: a revlew. J Environ Manag 92:407
38. Bulut Y, Gozubenli N, Aydm H (2007) Equilibrium and kinetics studies of adsorption of direct blue 71 from aqueous solution by wheat shells. J Hazard Mater 144:303